TRANSNAV International Journal on Marine Navigation and Safety of Sea Transportation
Volume 5 Number 1 March 2011

Assessing the Limits of eLoran Positioning Accuracy

J. Safar & F. Vejrazka
The Czech Technical University, Prague
P. Williams
The General Lighthouse Authorities of the United Kingdom and Ireland

ABSTRACT: Enhanced Loran (eLoran) is the latest in the longstanding and proven series of low frequency, LOng-RAnge Navigation systems. eLoran evolved from Loran-C in response to the 2001 Volpe Report on GPS vulnerability. The next generation of the Loran systems, eLoran, improves upon Loran-C through enhancements in equipment, transmitted signal, and operating procedures. The improvements allow eLoran to provide better performance and additional services when compared to Loran-C, and enable eLoran to serve as a backup to satellite navigation in many important applications. The Czech Technical University in Prague (CTU) participates in the eLoran research activities coordinated by the General Lighthouse Authorities of the United Kingdom and Ireland (GLAs). In our work we have focused on questions that arise when considering introducing new eLoran stations into an existing network. In particular, this paper explores the issue of Cross-Rate Interference (CRI) among eLoran transmissions and possible ways of its mitigation at the receiver end. An eLoran receiver performance model is presented and validated using an experimental eLoran signal simulator developed by a joint effort of CTU and GLAs. The resulting model is used to evaluate the achievable positioning accuracy of eLoran over the British Isles.

1 INTRODUCTION

In recent years, Global Navigation Satellite Systems (GNSS) have become an integral part of modern society. Be it on land, at sea or in the air, GNSS are an important and often the primary means of Positioning, Navigation and Timing (PNT). Although their qualities make them, in many aspects, superior to other PNT solutions, there is now broad agreement within the radionavigation community that satellite navigation systems are highly vulnerable to unintentional and intentional interference.

The concerns about the vulnerability of GNSS have sparked a renewed interest in the Loran PNT system, or rather in its upgraded version now widely called *enhanced Loran* or simply *eLoran*. The nature of the eLoran system makes its potential failure modes highly independent of GNSS. eLoran is a terrestrial system, which operates in the low-frequency band, uses high-power transmitters and completely different navigation signals. Its signals are also data modulated, which enables eLoran to deliver differential corrections, integrity messages and other data to users. Recently, considerable effort has thus been put into investigating whether eLoran can provide a viable backup to GNSS.

In Europe, the General Lighthouse Authorities of the United Kingdom and Ireland (GLAs) lead the way in eLoran research. The Czech Technical University in Prague (CTU) participates in the eLoran research activities coordinated by the GLAs. In our work we have focused on questions that arise when considering introducing new eLoran stations into an existing network. In particular, this paper explores the issue of *Cross-Rate Interference* (CRI) among eLoran transmissions and its impact on the positioning accuracy performance of eLoran.

In the first part of this paper we give a brief overview of the major factors that determine the achievable positioning accuracy of the system. We then report on the development of an experimental eLoran signal simulator and we demonstrate its use in assessing eLoran receiver performance under noise and interference conditions. Finally, a sample case study is presented that investigates the achievable

positioning accuracy of eLoran over the British Isles.

2 ACHIEVABLE POSITIONING ACCURACY OF ELORAN

When referring to accuracy of a positioning system, we need to distinguish between its absolute accuracy and repeatable accuracy. In (USCG COMDTPUB P16562.6), the *absolute accuracy* is defined as the accuracy of a position with respect to the geographic or geodetic coordinates of the Earth. The *repeatable accuracy*, then, is the accuracy with which a user can return to a position whose coordinates have been measured at a previous time with the same navigational system.

Due to the nature of low-frequency signal propagation, Loran systems may suffer from large measurement biases, resulting in absolute accuracy on the order of hundreds of meters. However, Loran's repeatable accuracy is comparable to that of single-frequency (L1) GPS. In the following we briefly discuss the major factors affecting the accuracy performance of eLoran and we explain how eLoran's absolute accuracy can be enhanced to the level of its repeatable accuracy.

2.1 *Factors affecting accuracy*

Unlike its predecessors, eLoran is a ranging system, which means that obtaining an accurate (2D) position fix generally requires:

1 Accurate Time-of-Arrival (ToA) measurements of signals from at least three transmitters,
2 Accurate ToA to range conversion,
3 Good geometry of the transmitters in view.

Transmitter geometry is a crucial factor in eLoran; however, the impact of geometry on the accuracy performance of a ranging system is well understood and will not be discussed in this paper.

Accurate conversion of ToAs to ranges from transmitters is hampered mainly by signal propagation irregularities when the signals travel over land. In eLoran we account for these irregularities by so-called *Additional Secondary Factors* (ASF). In order to achieve the best possible positioning accuracy, these correction factors in the area of interest need to be measured and stored in the receiver. Fluctuations in the ASF values should also be monitored and broadcast to the user in the form of differential corrections, e.g. using the eLoran data channel.

Table 1. Meeting the maritime accuracy requirement.

Accuracy Limiting Factor	Mitigation
Poor geometry	Installation of additional eLoran transmitters, perhaps using low power mini-eLoran stations as coverage gap fillers
ASF spatial variation	Detailed ASF maps stored in receivers
ASF temporal variation	Differential reference stations generating real-time corrections, broadcast to users e.g. by the eLoran data channel
Uncorrelated noise	Integration time ~ 5 sec is acceptable
Man-made noise and interference	Careful receiver antenna installation, advanced receiver signal processing

Accuracy of the ToA measurements themselves is a function of many variables. It is predominantly determined by the Signal-to-Noise Ratio (SNR) of the received signals. In the Loran frequency band, the dominant sources of noise are atmospheric noise, which is caused by lightning discharges, and man-made noise and local interference from, for example, switch-mode power supplies. Other sources of noise may include transmitter pulse timing jitter or receiver related noise.

Besides noise, another important source of ToA measurement error is interference caused by other radio signals. Currently the biggest source of interference to eLoran is eLoran itself, in the form of CRI. So what exactly is the cause of this interference?

eLoran transmitters are organised in groups of usually 3 to 5 stations called "chains" or "rates". The stations periodically broadcast groups of 8 or 9 specially shaped low-frequency, high-power, pulses (see Figures 2, 3). The interval between successive repetitions of the groups of pulses is unique to each chain and known as the *Group Repetition Interval* (GRI). Careful selection of GRIs and transmission times ensures that stations operating in a chain do not interfere with each other. However, the nature of the system is such that the signals from different chains overlap from time to time (see Figure 4) and may introduce errors into our ToA measurements – this is referred to as CRI.

Another effect of CRI is *transmitter dual-rate blanking*. As a legacy from the Loran-C era, some Loran transmitters are dual-rated, i.e. they broadcast signals on two GRIs. Such transmitters are periodically faced with the impossible requirement of radiating overlapping pulse groups simultaneously. During the time of overlap, those pulses of one group that overlap any part of the other group's blanking interval are suppressed (note e.g. the fourth group of pulses in Figure 2). The *blanking interval* extends

from 900 μsec before the first pulse to 1600 μsec after the last.

2.2 *Maritime eLoran*

Accuracy is the major factor affecting the suitability of eLoran for maritime navigation. IMO standards for the region of Port Approach specify a stringent accuracy requirement of 10 meters (95 percent of the time). A number of studies in the past have shown that accuracies better than 10 m are achievable (Basker et al. 2008, Johnson et al. 2007). Table 1 summarises measures that need to be taken in order to meet the 10 m accuracy requirement in the maritime environment.

From the above it follows that the major error sources in maritime eLoran are the residues of atmospheric noise, transmitter related noise, and CRI. While the impact of the first two factors is well understood and can be modelled (Safar et al. 2010), the issue of CRI has not been sufficiently described so far. In the rest of this paper we will therefore attempt to quantify the effects of CRI and provide CRI models for use in eLoran coverage prediction tools.

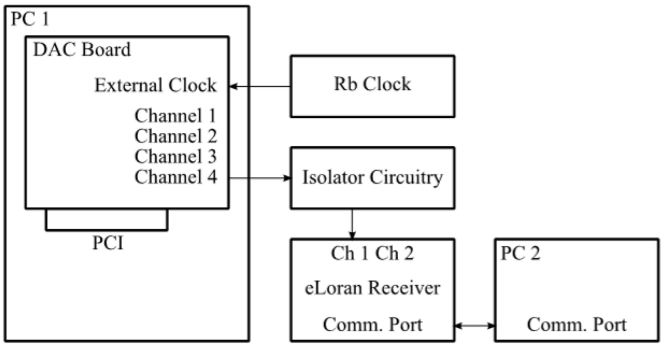

Figure 1. Schematic diagram of the GLA-CTU experimental eLoran signal simulator set-up.

3 ELORAN SIGNAL SIMULATOR

In order to meet the stringent eLoran accuracy performance standards, it is necessary that eLoran receivers employ special CRI mitigation algorithms (Safar et al. 2009). Quantifying the negative effects of CRI is therefore largely a receiver-oriented problem. Unfortunately (but not surprisingly), receiver manufacturers have not widely published the intricacies of their eLoran receivers. In order to get a better understanding of the performance of typical commercial eLoran receivers, an experimental eLoran signal simulator set-up is being developed through cooperation between the GLAs and CTU Prague. Using this set-up, it is possible to work with a receiver in a controlled environment and separate the negative effects of various error sources.

Figure 1 depicts the current simulator set-up. At the heart of the simulator is a DA converter board equipped with four 14-bit converters, providing us with four independent output channels each with a maximum analogue bandwidth of 52.5 MHz. The board is installed in a PC workstation (PC1) and communicates with the host system through the standard 32-bit PCI bus. In the current set-up a stable external 10 MHz clock signal from a GPS-disciplined Rubidium clock is supplied to the board.

The output of the board is connected to the antenna input of the receiver under test through a coupler, which galvanically isolates the receiver's input from the simulator and protects it from overloading. eLoran receivers can either use an E-field "whip" antenna or an H-field antenna. The latter typically consists of two loops whose outputs are combined in the receiver in software in order to provide a beam-steering capability. The simulator currently operates in the E-field (single-channel) mode only. The outputs of the receiver under test are monitored using a separate PC.

The simulator software currently allows the generation of ground wave and sky wave E-field signals, atmospheric noise, and simulation of the pulse timing jitter and transmitter dual-rate blanking. The parameters of the signals are either user defined or calculated for a specified location from corresponding propagation and noise models (Safar et al. 2010). In mathematical terms, the output signal of the simulator can be described as follows:

$$r(t)=\sum_{k=0}^{K-1}\sum_{m=0}^{M-1}\sum_{c=-\infty}^{\infty}\sum_{j=0}^{7}a_{mk}\,l\left(t-\tau_{mk}-jT_p-c\cdot T_{GRI,k}\right)\cdot \cos\left(\omega_0 t+\theta_{mk}+C_{kcj}\right)+n(t). \quad (1)$$

Here,

- K is the number of eLoran stations "in view" and $T_{GRI,k}$ are their respective group repetition intervals (in seconds);
- M - 1 is the number of sky waves considered, each with a different amplitude a_m, delay τ_m and phase θ_m ($m = 0$ represents the ground wave);
- C_{kcj} are the phase code values (0 or π, according to a standardised pattern), k is the transmitter number, c is the GRI number and j denotes the pulse number within a GRI;
- T_p T_p = 1 ms;
- ω_0 $\omega_0 = 2\pi\cdot 100\cdot 10^3$ rad/s corresponds to the eLoran carrier frequency of 100 kHz; note, that ω_0 is common to all stations;
- $l(t)$ represents the envelope of a single eLoran pulse; for $0 \le t \le 300$ μs it is given by Equation 2 and $l(t) = 0$ otherwise; t_p is the instant when the pulse reaches its maximum value, $t_p = 65$ μs;
- $n(t)$ is the noise waveform;

$$l(t) = \left(\frac{t}{t_p}\right)^2 \cdot \exp\left(2 - 2\frac{t}{t_p}\right). \quad (2)$$

Figures 2-4 show some example eLoran signal waveforms.

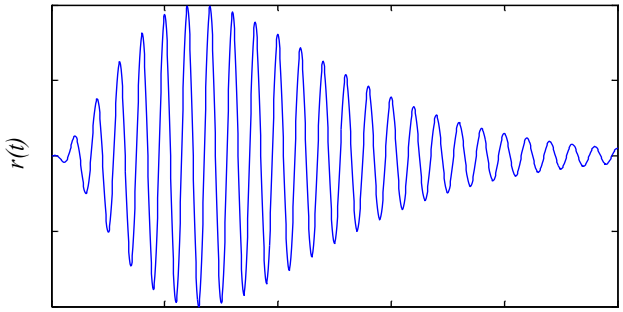

Figure 2. Ideal eLoran pulse (far E-field).

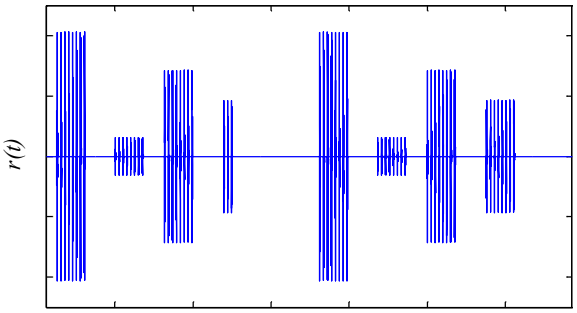

Figure 3. Simulated ground wave signals of GRI 6731 as would be received at Harwich, UK.

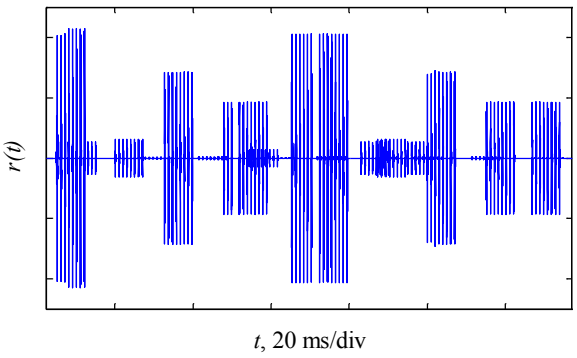

Figure 4. Simulated ground wave signals of all European chains as would be received at Harwich, UK.

There are no limitations to the number of chains or stations used in the simulation. The simulator therefore provides an excellent tool for studying the effects of CRI.

4 RECEIVER PERFORMANCE MODEL

As discussed earlier, positioning performance of a marine eLoran receiver is primarily determined by the errors in signal ToA measurements. In maritime eLoran, measurement biases are nearly perfectly eliminated through the use of ASF maps and differential corrections. In the following we therefore need be concerned only with the random fluctuations of the ToA error caused mainly by atmospheric noise and CRI, and we will use the standard deviation of the ToA measurements as our performance metric.

4.1 *Basics of eLoran receiver signal processing*

How does an eLoran receiver obtain a ToA measurement at the first place? The ToAs are measured in two stages. First, coarse signal delay relative to the origin of the receiver's time base is measured, based on the shape of the leading edge of the ground wave eLoran pulse. In the model of received signal represented by Equation 1 above, this delay is denoted τ_{0k}. When the approximate ToA is known, carrier phase of the eLoran ground wave signals, θ_{0k}, is measured which allows the receiver to calculate more accurate ToA values. The coarse estimates are only needed to resolve the ambiguity of the phase measurements; it is therefore the *carrier phase measurement error* which determines the accuracy of our ToAs, and which will be of interest in the following.

4.2 *Receiver performance in white Gaussian noise*

Let us first investigate the impact of atmospheric noise on our measurements. In the first approximation, atmospheric noise may be regarded as a white Gaussian stochastic process. We are therefore facing a problem of estimating the phase of a sinusoid embedded in White Gaussian Noise (WGN). This is a classical problem in estimation theory, and performance analyses of practical phase estimators typically reveal (see e.g. Hua & Pooi 2006) that the variance of the estimates is inversely proportionate to the SNR and the number of signal observations available. In case that the useful signal is a pure sinusoid, the SNR is simply defined as the ratio of the power of the sinusoid to the power of the noise in the signal samples. But how shall we define SNR of an eLoran pulse train?

4.2.1 *Defining SNR*

Unfortunately there is no universally accepted definition of SNR in eLoran; we propose a working definition to be used within this paper.

With conventional Loran signal processing the receiver uses, in the phase estimation process, one signal sample per each received pulse. Signal power can then be defined as the power of a sinusoid having the same amplitude as the envelope of the Loran pulse at the sampling point. There is a hitch, however. The position of the sampling point within the

pulse is a compromise between a low SNR at the beginning of the pulse and an increased probability of sky wave contamination later in the pulse; the position is dependent on the receiver's architecture and is generally unknown. Also, the pulse shape is distorted during propagation, reception and signal pre-processing at the receiver, which makes it even harder to determine the effective signal level at the sampling point.

To avoid possible ambiguities, we decided to define SNR external to the receiver. In our simulator experiments we are using the following definition: *SNR is calculated as the ratio of the power of the useful signal at the output of the simulator to the power of the radio-frequency noise present after filtering by the standard front-end filter (8^{th} order Butterworth, 3 dB bandwidth of 28 kHz, centred at 100 kHz).*

This definition assumes the use of ideal signal waveforms (see Equations 1, 2 above) and the power of the useful signal is calculated as the power of a sinusoid having the same amplitude as the ideal eLoran pulse envelope 30 µs into the pulse.

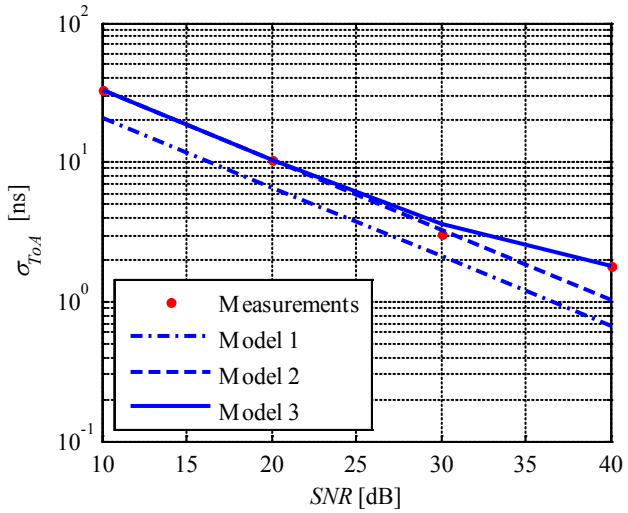

Figure 5. ToA standard deviation vs. SNR for eLoran signals in WGN.

In the performance analysis of a specific receiver we then need to bear in mind that the SNR seen by the receiver's phase estimation algorithms may differ from that above, e.g. due to signal distortion caused by the front-end filter.

4.2.2 *Developing the performance model*

Based on the cursory analysis above, we may assume that the ToA error model takes the form:

$$\sigma_{ToA}^2 = \frac{c_0 \cdot c_1}{N \cdot SNR}, \qquad (3)$$

where N is the number of signal samples used in the phase estimation process, SNR is expressed as a power ratio as defined above, $c_0 = (1.1254\ 10^{-6})^2$ takes account of the conversion from phase variance to ToA variance, and c_1 accounts for the pulse distortion during signal pre-processing. Estimated value of this constant for the Reelektronika LORADD receiver used in our analysis, based on information available to the authors, is $c_1 = (1.44)^2$.

Figure 5 shows the predicted ToA standard deviation as a function of SNR. Predictions according to Equation 3 are shown by the dash-dot line (Model 1). In this example it is assumed that the receiver is tracking a GRI 6731 signal and uses a 5 second averaging time, which gives N = 594 pulse samples per ToA measurement.

Also shown in Figure 5 are results of a simulator experiment conducted using the LORADD receiver and our prototype signal simulator (see also APPENDIX A). The actual ToA measurement errors turned out to be a little higher than our predictions. The offset can be calibrated out using another multiplicative constant, $c_2 = (1.55)^2$. The cause of this offset is unclear. The calibrated function is plotted as the dashed line in Figure 5 (Model 2).

It can also be seen from our measurements that the ToA vs. SNR characteristics flattens at high SNRs. This is presumably a result of the receiver's internal noise. The effect can be modelled using an additive constant, $c_3 = (1.5 \cdot 10^{-9})^2$ (solid blue line, Model 3). With the LORADD receiver, however, this effect occurs at very high SNRs unlikely to be encountered in practice, and can safely be neglected.

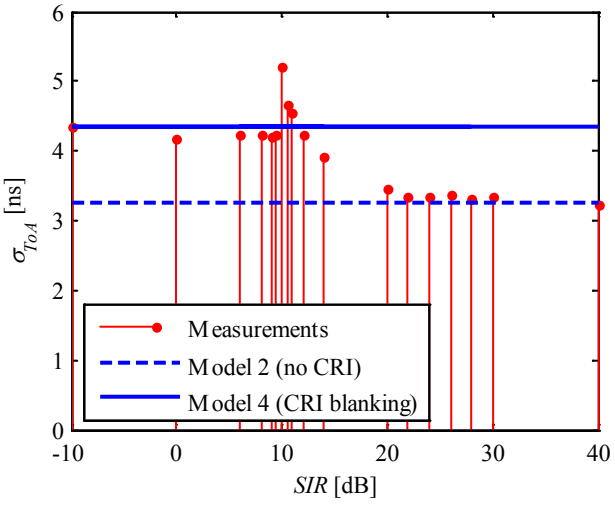

Figure 6. ToA standard deviation vs. SIR; GRI 6731 signal at SNR = 30 dB interfered with signals of GRI 7001 (M,X,Y). All the interfering signals in a particular experiment were set to the same level.

4.3 *Receiver performance under CRI conditions*

As mentioned before, in order to meet the stringent eLoran performance standards, the impact of CRI within the system must be greatly reduced. Several strategies concerning how the receiver can reduce the effects of CRI have been described in the literature (Pelgrum 2005). There are two prevalent CRI mitigation techniques, commonly referred to as *CRI cancelling* and *CRI blanking*.

eLoran employs all-in-view receivers capable of simultaneously tracking signals of many rates. When an eLoran signal is being tracked, a footprint of the received pulse waveform is available. With cancelling, the receiver uses this footprint to reconstruct accurate replicas of the individual signals and suppress the signals of all unwanted rates (Estimate & Subtract). This allows the receiver to mitigate the effects of CRI almost perfectly, however the technique has its limitations, as will be shown shortly.

With CRI blanking, the receiver detects the pulses likely corrupted by CRI and discards them. The interference is thus completely suppressed, but the price we pay is a (sometimes excessive) loss of tracking energy.

4.3.1 *Simulator experiments*

In order to assess the effects of CRI on a modern eLoran receiver, a series of simulator experiments were conducted in which signals of a selected chain were disturbed by white Gaussian noise and interfered with signals of another chain at different levels. Figure 6 plots the ToA standard deviation versus the Signal-to-Interference Ratio (SIR) for a GRI 6731 signal at 30 dB SNR, interfered with the signals of GRI 7001.

We can see from the plot that for high enough SIR values, the errors are largely determined by the Gaussian noise (see the dashed line in Figure 6, Model 2) and can easily be modelled as described in the previous subsection.

As the interference grows stronger, the measurement errors gradually increase. This gradual increase suggests that in the region of relatively weak interference (SIR above 10 dB) the receiver is using some kind of cancelling algorithm to mitigate CRI. Since the signal replicas used in the CRI cancelling process are mere estimates of the true interfering waveforms, there is always some residual effect on our ToA measurements. This effect is more pronounced as the SIR decreases. With SIR values approaching 10 dB the residual error rises sharply and when the SIR is further decreased, the receiver apparently switches to CRI blanking. A model for the transitional region is currently being developed and will be presented in a follow-up paper. We will now concentrate solely on the CRI blanking.

4.3.2 *Modelling the impact of CRI blanking*

As explained above, with CRI blanking all the colliding pulses are completely removed from the signal processing. The task of quantifying the impact on the ToA measurements thus reduces to estimating the percentage of discarded pulses and decreasing accordingly the number of samples per ToA measurement in Models 1 to 3 above.

In the following considerations we will ignore the influence of the ninth master Loran pulse, as well as any data modulation of the signals. We will assume that the receiver uses the same blanking strategy as is used on Loran dual-rated transmitters, i.e. that it discards all pulses that overlap any part of the blanking interval of the cross-rating pulse groups (see Figure 7). This is a different approach from the one in our previous paper (Safar et al. 2010), where we had assumed that blanking only occurred when individual pulses overlap each other.

Let us first consider the case of two interfering eLoran ground wave signals. It can easily be shown (Safar et al. 2009) that the average portion of blanked pulses of the desired signal, or the *blanking loss*, can be calculated as:

$$L_b = \frac{w_d + w_i}{T_{GRI,i}}, \tag{4}$$

where w_d is the pulse width for the desired signal, w_i is the width of the blanking interval for the interfering signal, and $T_{GRI,i}$ is the length of the group repetition interval of the interfering station. In our analyses we set $w_d = 250$ µsec, and $w_i = 9500$ µsec.

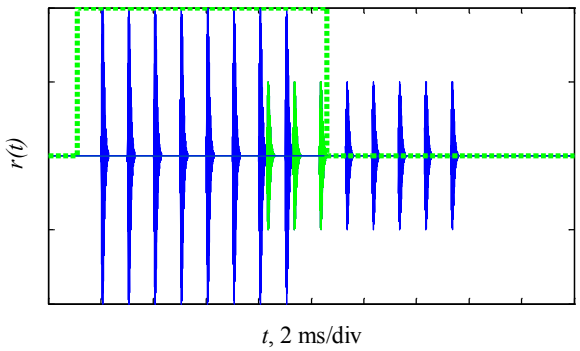

Figure 7. CRI blanking. Dashed line shows the blanking interval extending over the pulse group of the unwanted cross-rating signal. In this example, samples of the first three pulses of the second group will be discarded.

When analysing real-world eLoran systems we also need to evaluate the *blanking loss due to multiple cross-rating stations*, $L_{b,rx}$. In this case, the evaluation needs to be broken down into two stages. First, we calculate the blanking loss due to stations of individual GRIs, $L_{b,rx,gri}$, by summing the contributions of individual stations, operating on a given

GRI. In the following, g denotes the GRI of the interfering station, s identifies individual stations in view, and S_g is the set of stations operating on GRI g:

$$L_{b,rx,gri}[g] = \sum_{s \in S_g} L_{b,rx,st}[s]. \quad (5)$$

Simply summing the blanking loss values is justified, as signals of multiple interferers from a common chain cannot overlap.

Second, we assume that the effects of interference from stations operating on different GRIs are statistically independent, which allows us to calculate the resulting blanking loss as:

$$L_{b,rx} = 1 - \prod_{g} \left(1 - L_{b,rx,gri}[g]\right). \quad (6)$$

In addition to ground wave, the effect of *sky wave borne CRI* also needs to be taken into account. The presence of sky waves increases the probability of collision between the interfering pulse trains, depending on the sky wave delay. We model this effect by increasing the width of the blanking interval w_i by the estimated sky wave delay at the point of signal reception.

As mentioned earlier, there is also a loss of signal due to *dual-rate blanking*. In Europe, dual-rated transmitters use priority blanking, where the same rate is always blanked at every overlap (the priority rate is not affected). The loss due to transmitter blanking, $L_{b,tx}$, can then be easily calculated using Equation 4.

The *total blanking loss* for a particular signal of interest, including the effects of dual rate transmitter blanking, $L_{b,tot}$, can be found in a similar fashion as above:

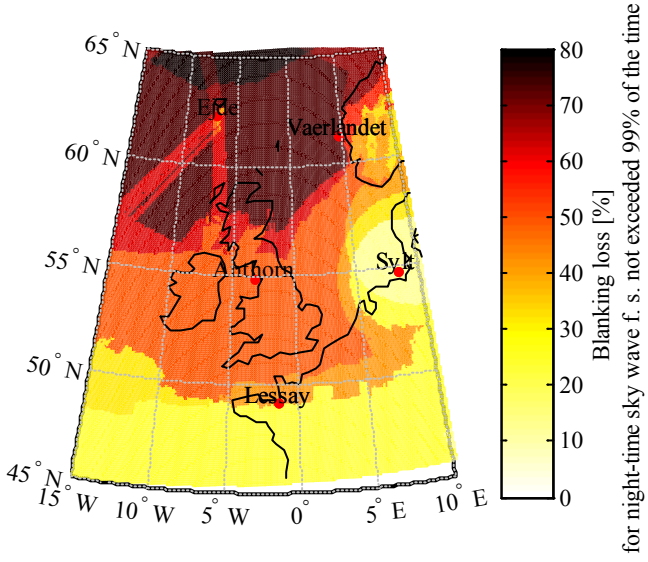

Figure 8. Blanking loss for the 6731 Sylt rate under worst-case sky wave conditions expected.

$$L_{b,tot} = 1 - \left(1 - L_{b,tx}\right) \cdot \left(1 - L_{b,rx}\right). \quad (7)$$

The impact of CRI blanking on the ToA measurement error for a signal of a particular station received at a given SNR can then be estimated using one of the models presented in Subsection 4.2.2, where the number of averaged pulses, N, needs to be reduced accordingly, i.e. we use $(1 - L_{b,tot}) \cdot N$ instead of N. With this modification to the model, we achieve nearly perfect agreement with our measurements (see Figure 6, Model 4).

5 CASE STUDY

We will now demonstrate the use of the models presented in this paper through a case study investigating the achievable positioning accuracy of eLoran over the British Isles. Our transmission network will be formed by the 14 transmissions from the 9 European transmitters currently in operation, configured according to Appendix B.

In our study we have made use of the GLA coverage and performance model (Safar et al. 2010) which provides estimates of ground wave and sky wave signal parameters and atmospheric noise values over the area of interest. In accordance with common practice (Last et al. 1991), we have used annual atmospheric noise not exceeded 95% of the time, and night-time sky wave field strength values at 99 percentile, providing a conservative estimate of own sky wave interference. The height of the ionosphere has been assumed to be 91 km.

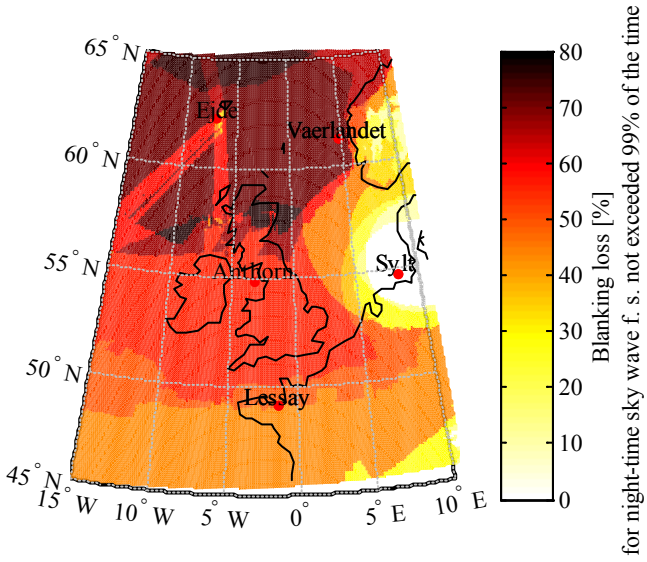

Figure 9. Blanking loss for the 7499 Sylt rate under worst-case sky wave conditions expected.

ToA measurement errors for individual stations have been estimated using the receiver performance models described in Section 4. The signal averaging

time has been assumed to be 5 seconds – a typical value for a marine receiver. The receiver is assumed to acquire and track a signal of a particular station only if the SNR is higher than 0 dB (BS EN 61075:1993) and the sky wave field strength to ground wave field strength ratio and sky wave delay are within the limits prescribed by the receiver Minimum Performance Standard (BS EN 61075:1993). CRI at SIR values higher than 10 dB has been assumed to be perfectly cancelled (Model 2); interfering signals at SIR lower than 10 dB and SNR above 0 dB have been blanked (Model 4). *SIR* in our CRI analysis has been defined as the ratio of the power of the ground wave of the useful signal to the power of the interfering signal, calculated either from the ground wave or the sky wave field strength (whichever is higher). As an example of the expected effects of CRI, Figures 8, 9 show the estimated blanking loss for both rates of the dual-rated transmitter at Sylt.

Finally, based on the predicted ToA measurement errors and transmitter geometry, positioning errors have been estimated as described in our previous paper (Safar et al. 2010). Figure 10 shows the predicted 95 percent radius (R95) accuracy calculated under the assumption of Gaussian-distributed measurement errors. As explained above, the plot also assumes that differential eLoran and ASFs are available over the entire area.

6 KNOWN ISSUES & FUTURE WORK

There are a number of reasons why the figures presented in this paper should be interpreted with caution. Let us briefly mention the most important ones.

First of all, we still do not have a rigorous definition of SNR in eLoran. It is therefore difficult to compare measurements obtained using different receivers, and also to translate SNR values from coverage prediction models to actual SNRs as would be seen by a practical receiver. This issue is currently being discussed within the Radio Technical Commission for Maritime services - Special Committee 127 on eLoran Systems (RTCM SC-127).

In developing our receiver performance model we have approximated atmospheric noise by Gaussian-distributed noise. It is well known that real atmospheric noise also contains an impulsive component. eLoran receivers, if properly designed, can benefit from that and may achieve substantial processing gain by suppressing the impulsive part of the noise. In real atmospheric noise conditions, the receiver may therefore perform better than our model predicts. Quantifying the achievable processing gain, however, requires knowledge of the amplitude distribution of the noise (Boyce 2007).

Further performance improvements may be achieved through sky wave aided tracking. Simulator experiments could be conducted to verify this. We might also want to explore alternative sky wave propagation models, such as the USCG-Decca model (Last et al. 1991) which was specifically designed for the Loran frequency band.

On the other hand, there are a number of factors that haven't been considered and may negatively impact the tracking performance. These are for example residual errors due to CRI cancelling, background CRI from distant stations that cannot be tracked, residual Carrier-Wave Interference, or the impact of transmitter timing jitter. These factors may be important at high SNRs.

Finally, we might also want to include differential eLoran in the model. This requires a study of spatial decorrelation of the differential corrections as the user receiver moves away from the reference station. Also the accuracy of ASF maps used in user receivers needs to be assessed and included into the overall error budget.

7 CONCLUSIONS

We have studied the tracking performance of a typical commercially available eLoran receiver under Gaussian noise and CRI conditions. Based on our findings we have developed an updated receiver performance model for the purpose of coverage prediction and optimisation.

Using this new model we have analysed the possibility of mitigating CRI within the European transmission network through blanking at the receiver end. Our analysis suggests that with the current configuration of the network, blanking results in a substantial loss of tracking energy, and we recommend that a study is conducted to examine the potential gains of redesigning the timing of the (e)Loran transmissions in Europe.

We have also used the updated receiver model to generate a positioning accuracy plot for the GLAs' service area. Despite the relatively high blanking loss values assumed in the analysis, the plot suggests that sub-10 m accuracy with eLoran should be achievable in areas of good transmitter geometry, such as off the north and east coast of Britain. *The performance figures presented herein should, however, be interpreted with caution, as this is still work in progress.*

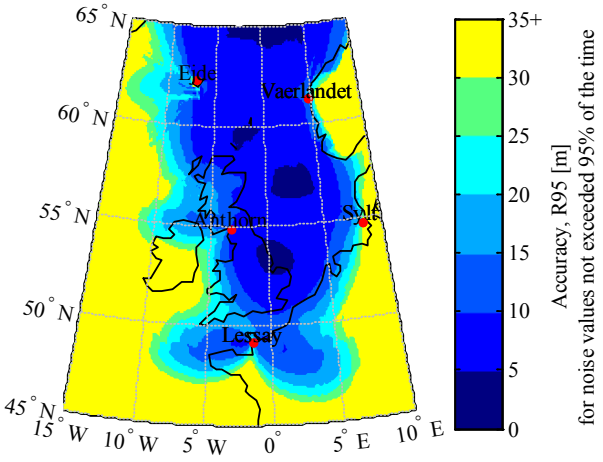

Figure 10. Achievable positioning accuracy of eLoran (R95) under worst-case sky wave conditions expected.

ACKNOWLEDGEMENTS

This work has been supported by the General Lighthouse Authorities of the United Kingdom and Ireland.

REFERENCES

Basker, S. et al. 2008. Enhanced Loran: real-time maritime trials. In *Proceedings of Position, Location and Navigation Symposium, 2008 IEEE/ION.*

Boyce, C.O.L. 2007. *Atmospheric noise mitigation for LORAN*. PhD thesis, Stanford University.

BS EN 61075:1993. *Loran-C receivers for ships - Minimum performance standards - Methods of testing and required test results*, British Standards Institution.

Hua, F. & Pooi Y. K. 2006. ML estimation of the frequency and phase in noise. In *Global Telecommunications Conference, 2006. GLOBECOM '06. IEEE*.

Johnson, G. et al. 2007. Navigating harbors at high accuracy without GPS: eLoran proof-of-concept on the Thames river. In *Proceedings of ION National Technical Meeting*, San Diego, CA, 22-24 January, 2007.

Last, D. et al. 1991. Ionospheric propagation & Loran-C range - the sky's the limit. In *Proceedings of the 20th Annual Technical Symposium, Wild Goose Association*, Williamsburg, VA, 1-3 October, 1991.

Pelgrum, W. 2005. Noise - from a receiver perspective. In *Proceedings of the 34th Annual Convention and Technical Symposium of the International Loran Association*.

Safar, J. et al. 2010. Accuracy performance of eLoran for maritime applications. *Annual of Navigation*, 16:109–122.

Safar, J. et al. 2009. Cross-rate interference and implications for core eLoran service provision. In *Proceedings of the International Loran Association 38th Annual Meeting*, Portland ME.

US Coast Guard COMDTPUB P16562.6 1992. *Loran-C user handbook*.

APPENDIX A NOTES ON MEASUREMENTS

In our experiments we have been using the Reelektronika LORADD receiver updated with a new firmware developed by Plutargus (v. 1.0), running in the E-field mode.

The LORADD receiver is not capable of measuring absolute ToAs, as it is not equipped with an atomic clock. Instead, we can measure Time Differences (TD) between two selected signals and thus remove the common clock drift. Note, however, that the error in the TD measurements is a combined error, composed of errors of both the signals used in that measurement. In our experiments we have compensated for this effect mathematically.

We have used 1000 seconds worth of data to calculate the tracking errors in Figures 5, 6.

APPENDIX B

Table B.1: European Loran stations.

GRI ID and station name	Dual-rate blanking
6731 Lessay	Priority 6731
6731 Soustons	Not dual-rated
6731 Anthorn	Not dual-rated
6731 Sylt	Priority 7499
7001 Bø	Priority 9007
7001 Jan Mayen	Priority 9007
7001 Berlevag	Not dual-rated
7499 Sylt	Priority 7499
7499 Lessay	Priority 6731
7499 Værlandet	Priority 7499
9007 Ejde	Not dual-rated
9007 Jan Mayen	Priority 9007
9007 Bø	Priority 9007
9007 Værlandet	Priority 7499